

Map-Z: Exposing the Zcash Network in Times of Transition

Erik Daniel

*Distributed Security Infrastructures
Technical University of Berlin
erik.daniel@tu-berlin.de*

Elias Rohrer

*Distributed Security Infrastructures
Technical University of Berlin
elias.rohrer@tu-berlin.de*

Florian Tschorsch

*Distributed Security Infrastructures
Technical University of Berlin
florian.tschorsch@tu-berlin.de*

Abstract—Zcash is a privacy-preserving cryptocurrency that provides anonymous monetary transactions. While Zcash’s anonymity is part of a rigorous scientific discussion, information on the underlying peer-to-peer network are missing. In this paper, we provide the first long-term measurement study of the Zcash network to capture key metrics such as the network size and node distribution as well as deeper insights on the centralization of the network. Furthermore, we present an inference method based on a timing analysis of block arrivals that we use to determine interconnections of nodes. We evaluate and verify our method through simulations and real-world experiments, yielding a precision of 50 % with a recall of 82 % in the real-world scenario. By adjusting the parameters, the topology inference model is adaptable to the conditions found in other cryptocurrencies and therefore also contributes to the broader discussion of topology hiding in general.

Index Terms—Zcash, blockchain, P2P, topology inference

I. INTRODUCTION

Since Bitcoin’s [1] introduction in 2008, a large number of so-called altcoins emerged. Altcoins are inspired by the general principle of a distributed ledger, but aim to improve the system design in one way or another. One of these altcoins is the Zcash project, which implements the Zerocash payment scheme [2]. Zcash launched in October 2016 and aims to enable anonymous, yet publicly verifiable, transactions by employing zero-knowledge proofs [3].

To date, most research on Zcash concentrates on anonymity and security aspects of the ledger [4, 5]. Another central aspect of the system, however, has not yet been considered in prior investigations: the Zcash peer-to-peer network. This is particularly notable, since it has been shown before that the properties of the networking layer may have serious consequences on the security and privacy of blockchain-based systems [6, 7]. Moreover, revealing the network topology may render even the best privacy-preserving cryptographic primitives ineffective, if it is possible to link transactions and blocks to specific peers [8, 9]. On a general note, monitoring the network status and health can indicate arising issues, such as a high degree of mining power centralization. This sort of centralization can be considered critical as it puts the majority of computational resources in the hands of a single entity, which could empower a malicious actor to rig the consensus in her favor. Centralization in general undermines the goal of distributed trust since the payment history could be altered at any time [1].

In this paper, we provide the first longitudinal measurement study of the Zcash peer-to-peer network and present a model for topology inference. In our measurement study, we expose information about Zcash nodes and their connectivity. To this end, we observed the Zcash peer-to-peer network from a vantage point over a period of four month (July to October 2018), covering multiple major client and protocol updates.¹ The vantage point is a deployed reference client, modified for data collection. The empirical data allows us to conduct a global analysis of the Zcash network, capturing key metrics such as network size, block propagation behavior and timing, mining power distribution, and node churn. We also use the data to reveal information about the nodes themselves, including client version and global node distribution.

Based on the measured data of the Zcash network and previous ideas for topology inference in the Bitcoin network [10], we developed a passive topology inference method which exploits the block relay mechanism. While our method allows us to infer connections of mining nodes and their direct neighbors only, it otherwise has a number of advantages: It is independent of countermeasures for active timing analyses based on transactions, such as trickling or diffusion spreading [9]. Additionally, the usage of blocks as a basis for inference produces no costs in terms of transaction fees. We verify our model in a simulation using the Boost Graph Library [11] and present various ways to determine the parameters of our model. Moreover, we test the approach in a series of real-world experiments with two Zcash network nodes. In this scenario, the model could achieve a precision of 50 % and a recall of 82 %, proving its applicability in a real-world setting. In general, we were able to reproduce and improve the results of [10]. As the topology inference model is adaptable to the protocol specifications of other cryptocurrencies, it contributes to the discussion of topology hiding in general.

The rest of the paper is structured as follows. Section II shows similar research concerning characterization and topology inference of cryptocurrencies. Section III presents our research of the Zcash peer-to-peer network. In Section IV, we introduce our inference model which is evaluated in Section V. Section VI concludes the paper.

¹The measurement data and simulation code base is publicly available at https://gitlab.tubit.tu-berlin.de/erik_1105/map-z_data

II. RELATED WORK

So far, most research in the field of cryptocurrencies concentrates on Bitcoin and Ethereum: prior contributions [12, 13, 14] explored both networks and collected statistical data by deploying measurement nodes. Among others, they observed that the block propagation delay has a significant impact on the security and fairness of the consensus layer. This has also been studied analytically and with the help of simulations [6, 7]. In [15], the degree of centralization of Bitcoin and Ethereum is investigated. The authors found both networks to be highly centralized in terms of (geographical) mining power distribution. As also shown in [16], the mining power distribution is dominated by Chinese mining pools, which bears the risk of intervention by a state actor. Moreover, the authors argue that the interference of the so-called “Great Firewall of China” leads to degraded block propagation performance in the Bitcoin network.

Beyond Bitcoin and Ethereum, Zcash exhibits similar properties to Bitcoin but provides additional privacy guarantees by implementing so-called shielded transactions, which use zero-knowledge proofs [3] to yield anonymous transactions. Most prior work on Zcash focuses on the anonymity aspects. In [4], the authors studied the effectiveness of the anonymity features in Zcash by analyzing the shielded function usage patterns. Similarly, the authors of [5] analyzed the data stored in the Zcash blockchain to evaluate its anonymity. However, to the best of our knowledge, no previous work studied the network behavior of Zcash. Our work therefore provides the first measurement study concentrating on Zcash’s peer-to-peer networking layer.

Network tomography in general comprises methods to infer internal network characteristics, including topology inference. The methods basically differ in the employed type of probing technique, which boils down to either unicast or multicast measurements. While unicast measurements, such as sandwich probes [17] or RTT measurements [18], are hard to realize in Zcash, as the observer cannot determine the spreading path, multicast measurements are easier to reproduce. Most approaches using multicast measurements, e.g., [19], use end-to-end loss instead of delay, though. Since loss rates can only be measured between two peers, these approaches are not applicable in Zcash as well.

There exists research that concentrates on topology inference of cryptocurrencies: Miller *et al.* [20] use the timestamps of announced IP addresses to infer links between different nodes and also try to find mining pools and influential nodes. Another approach by Grundmann *et al.* is primarily used to expose only a few targeted nodes. The approach uses a method to detect the topology of Bitcoin by exploiting its transaction propagation mechanics [21].

In [10], Neudecker *et al.* present a method to infer the topology of a peer-to-peer flooding network like Bitcoin with the help of an analytical model. The authors list in [22] topology hiding as a security requirement for blockchain networks and present an adversary model which tries to

infer the topology based on the peer discovery mechanism. Furthermore, they show the importance of the transaction relay delay as a countermeasure against topology inference. The ideas of both papers serve as the basis for the conducted topology inference. In this paper, our inference model however extends the approach by employing a passive, cost-efficient monitoring, and more accurate approach, promising to capture the whole network.

III. MAPPING THE ZCASH NETWORK

In this section, we present results of our measurement study of the Zcash network. The goal of this investigation is to illuminate network characteristics on a global scale. To this end, the empirical data covers two main categories: data about individual nodes and about information propagation between nodes. In particular, we show the worldwide interest in Zcash and present insights on network size and stability, geographic node distribution, software deployment and lifecycles, origin of blocks, block propagation time, as well as mining centralization.

A. Measurement Setup

In order to characterize the Zcash network, we deployed a Zcash reference client for data collection as an observation point. The client was run on a virtual machine in our university network (TU Berlin, IPv4). However, minor client modifications were necessary to ensure a reliable measurement setup that avoids unwanted side-effects and yields representative results. For example, in order to get a comprehensive overview, it is necessary that the observation point is connected to as many peers as possible. We therefore increased the maximum number of outbound connections and allowed for 873 simultaneous connections, which is the upper limit provided by the reference client on a Linux machine. Moreover, we disabled the sending of block inventory messages that announce new blocks to peers. We however recorded arrival times of block inventory messages from neighboring peers to get an overview of the block propagation times in the network. Additionally, we recorded information about connected peers and the mining difficulty. In our measurements, we omitted all data points recorded during the initial blockchain download, because this is a one-time phase and therefore does not represent normal operation. The described methodology is on par with other measurement studies [23].

We recorded data snapshots about peers and blocks every five minutes and two minutes, respectively. While a time interval of two minutes does not guarantee to record every single block, it should capture the vast majority of blocks². In addition to the application layer data, we sent ICMP ping messages to the connected peers, which serve as a baseline and help to reveal networking problems during the measurements.

Our measurement period spans from July 2, 2018 until November 12, 2018. It thus captures the time after Zcash’s first network upgrade called “Overwinter” [24]. During the

²At the time of writing, Zcash’s block interval time is 2.5 minutes

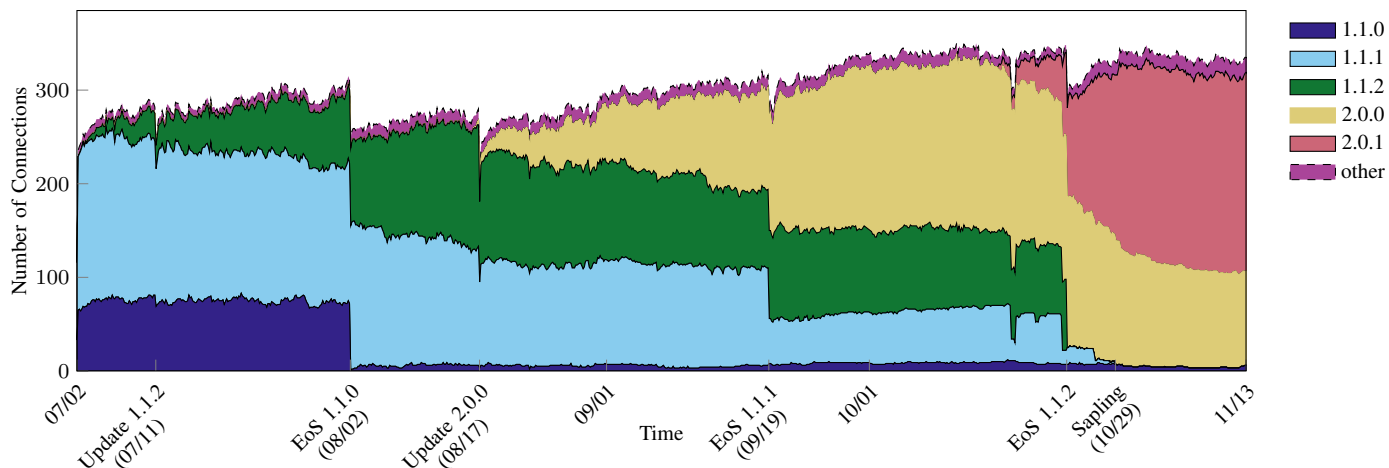


Fig. 1: Distribution of announced version strings in the Zcash peer-to-peer network.

measurements, we upgraded the client twice to include new functionalities and to ensure compatibility after Zcash’s second network upgrade called “Sapling” [24]. Accordingly, client versions MagicBean 1.1.1, 1.1.2, and 2.0.0 were utilized.

B. Measurement Results

Network size and client versions: To begin with, we are interested in the network size and the number of nodes running a specific software version. In order to estimate these numbers, we count the number of network peers that were connected to our measurement node over time.

The number of simultaneous connections held by our vantage point and the distribution of client versions are shown in Fig. 1. As the number of observed simultaneous connections never exceeds this range, we estimate the size of the network to be around 300 to 350 nodes. Note however that we observed 4,208 distinct IP addresses which established a connection to our vantage point at least once. In total, the address manager of our node learned from exchanged address information about around 25,000 IP addresses. We assume that this high number of (stale) IP addresses stems from a small number of network peers that constantly change their IP address.

As a side note, on November 11, we observed 117 simultaneous connections coming from the same IP address. These 117 connections were open for approximately 30 minutes but did not send any data. The version name of this client was “xbadprobe”, which suggests that this may have been an attempt to occupy the node’s inbound connections.

The reference client provided by the Zcash developer team uses the string “MagicBean” followed by a version number as the client name. While it is possible to modify the client software without changing the announced version string, we consider this a negligible side-effect and use the strings to account for different client versions. Likewise, the data shows that only a small fraction of clients use custom version strings or minor versions. We therefore only consider major client versions and categorize minor versions (e.g., 2.0.1-rc1) and custom version strings as “other clients” in the following.

Since client version 1.0.9, each reference client comes with an End-of-Support (EoS) period, which causes the client software to halt after the EoS period has expired. At the time of writing, the period is set to be 64,512 blocks or approximately 16 weeks. Visually, we can clearly identify the EoS periods in Fig. 1. For example, we captured the complete 16 week lifecycle for client version 1.1.2, showing the adoption of and transition to other versions. Moreover, client versions older than 1.1.0 are no longer supported after the second network upgrade. Connections to these outdated clients are therefore dropped after the version handshake. Nevertheless, our data reveals that some clients were still active with older client versions, even though they no longer supported the consensus. However, the client versions 1.1.0 and 1.1.1 included a configuration option which disabled the automatic halt after the EoS period, which explains why the observed drop in numbers for those versions is not as entire as for version 1.1.2. The introduction of EoS periods is an interesting and clearly effective approach to ensure that all users update their client software and obsolete versions leave the network in a timely manner. This reduces the threat that bugs persist even after they were already fixed, which in turn bears the danger to undermine the trust in the currency.

Geographical and mining distribution: In Fig. 2, we show the country distribution of observed IP addresses and block origins during our measurement period, which provides insights on Zcash’s global adoption and mining power distribution. We used GeoIP [25] to map the IP addresses from our data set to countries. If a country had less than 30 IP addresses it is grouped as “other”. We further assume that the host which first announces the block is also the block’s miner.

We generally can see that the Zcash network spreads over all northern continents. From a country perspective, the clients are mainly present in Russia and the United States. From a continent perspective, however, the network is evenly distributed over Europe, America, and Asia. Only a small number of nodes are located in the southern continents.

In contrast, the mining power distribution clearly shows a

skewed distribution, suggesting an immense centralization of mining power. We observe that around 51 % of the blocks are created by 16 miners, out of which ten are located in China. Overall, 53 % of all observed blocks originate from China, 10 % from France, 9 % from the United States, 5 % from Germany, and 4 % from the Netherlands. The remaining 19 % are from different countries. Notably, while we observed only seven IP addresses from Ireland, the country contributes 3% of all blocks. It should also be mentioned that we found some nodes that did not announce any blocks.

We also observed a quadruplication in the difficulty during our measurements, resulting from an increased mining power, which effectively raises the bar to start mining blocks in the Zcash network. This increase in mining power hence makes it unlikely that the country distribution of miners will change in the near future. As new Equihash-capable ASIC mining hardware was introduced in mid 2018, the increase in mining power is likely a result of a gradual change from GPU mining to ASIC mining.

In general, geographical centralization of mining power in one jurisdictional area creates the risk of interference by a state actor. The centralization of mining power in China we observed is in line with results from other cryptocurrencies, e.g., Bitcoin [16].

Block propagation: In order to determine the time it takes for a block to propagate in the network, we measured the time it takes until a block is announced by all neighbors of our vantage point. Fig. 3 accordingly shows the time differences as a mass function of the first and all following observed block announcements (i.e., arrival of block inventory messages). In order to estimate when the neighbor peers learned about the blocks, the shown times are adjusted by subtracting half RTT retrieved from Zcash’s keep-alive messages. The RTT is estimated using the exponential weighted moving average (EWMA) approach known from TCP (cf. RFC 6298).

We note that block propagation follows a long-tailed distribution, where a considerable number of inventory messages take significantly longer. After 690 ms, 50 % of all block inventory messages have arrived. And after two seconds, 90 % of all nodes know the block. Furthermore, it takes a small number of nodes a really long time to retrieve and propagate new blocks. Interestingly, this is in accordance with similar observations ($\approx 2 s$ for 90 % coverage) made in [23] for the Bitcoin network, even though the latter is considerably larger (at the time of this paper: ≈ 350 vs. ≈ 10.000 nodes).

In general, we can say the network needs around 700 ms for a block to be known by most peers and roughly two seconds to spread the information in the whole network. However, this delay does not seem to have a significant negative impact on consensus. From the 57,365 observed block hashes, only 297 are not included in the Zcash blockchain, yielding a stale block rate of 0.337 %. This measurement is comparable to the stale rates found in other cryptocurrency networks like Bitcoin or Litecoin, which according to [7] exhibited around 0.41 % and 0.273 % stale blocks, respectively.

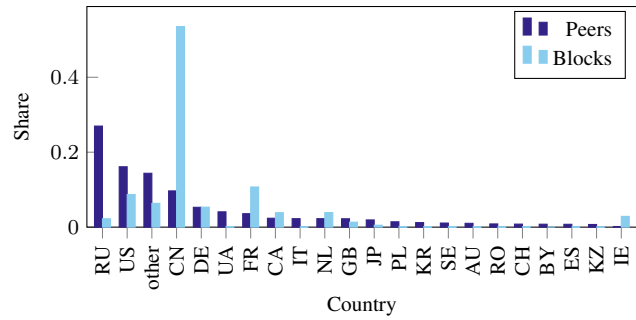


Fig. 2: Distribution of observed addresses and block origins.

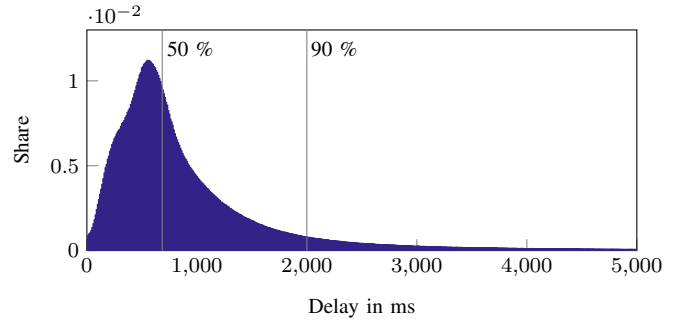


Fig. 3: Block inventory arrival time differences.

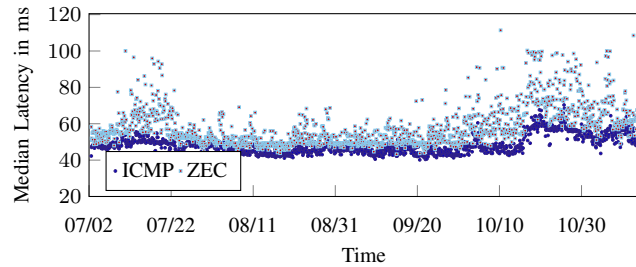


Fig. 4: Latencies of the connected clients.

Network stability: Lastly, we are interested in the network load and stability. Fig. 4 shows the median latencies to all connected nodes over time. As a baseline, we additionally measured ICMP ping times and compare them to the Zcash ping measurements. The Zcash ping is a keep-alive message, scheduled every two minutes, which is sent to all neighbors via the respective TCP connection and is usually processed with all other exchanged messages. This leads to head-of-line blocking during transaction and block relay, whereby the Zcash ping messages are delayed. In comparison to the more reliable ICMP ping, it therefore rather serves as an indicator of a node’s activity.

The ICMP ping’s median values vary between 45 ms and 55 ms and are lower and less fluctuating than Zcash pings. From October 18, the median ICMP ping and Zcash ping latencies increased. This behavior could be a reaction to the second upgrade (“Sapling”). In this upgrade, the performance of the so-called shielded transactions was improved, which might have made them more attractive and could have led to increased usage. The increase of the ICMP ping could also be due to network interferences in the University network.

As in any other open peer-to-peer network, nodes in the

Zcash network can join and leave at any time, which results in an ever-changing topology. In order to assess the network stability, we analyzed the lifetime of connections. In order to circumvent artificial spikes in our data set stemming from our own client updates, we only consider the time after we updated our measurement node to client version 2.0.0.

We generally observed that around 50% of connections remained active for at least 50 minutes. Moreover, around 20% of connections lasted longer than a day, while 10% were active for more than four days, and 1% have even remained active since the beginning of our study. We also observed around 24% of short-lived connections, which were active less than five minutes. In summary, we could see that a good part of the network consists of long-lived stable peers. This *core network* can certainly become a reasonable target for topology inference.

IV. TOPOLOGY INFERENCE

In the following, we aim to infer the interconnectivity of Zcash network peers by conducting a passive timing analysis, which allows us to incrementally uncover the topology of the peer-to-peer network. To this end, we build upon and extend the inference model developed by Neudecker *et al.* [10, 22]. We however replace the employed active transaction measurements with passive block measurements, which, as we will see, has a number of advantages. In a nutshell, the goal is to infer the connection between two peers by monitoring when they emit inventory messages announcing new blocks. The model concentrates on detecting connections between peers adjacent to mining nodes, which can be used to reveal security-critical information of the network.

A. Inference Model

Let us assume a source node S , which we consider the origin of a block, and a relay node R . Moreover, assume that node S and R are both interconnected and also connected to a measurement node M .

A schematic of this three-node scenario is shown in Fig. 5. While numbered arrows indicate the order and direction in which messages are sent, dashed arrows indicate further protocol messages that are however only shown for completeness, but do not influence the inference model. Hence, a block relay in Zcash consists of a three-way message exchange (announce, request, response): An `inventory` message announces a block, a `getdata` message requests the block, and a `block` message transmits the actual block data.

From the perspective of M , we have knowledge about the time node S and R announced a specific block to node M . We also know the round-trip times RTT_{MS} and RTT_{MR} between nodes M and S , as well as nodes M and R , respectively. The measured arrival times consist of at least a delay introduced by the latency between S and R and the processing delay of R . Since the measurements are conducted on M , the measured time includes $RTT_{MS}/2$ as well as $RTT_{MR}/2$, which we subtract once prior to the following calculations. Note that if the latency difference is “small enough”, S and R are directly

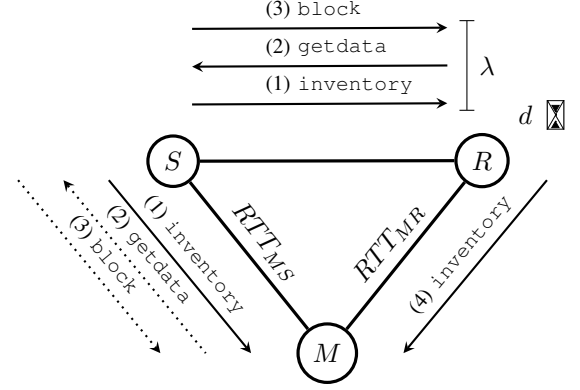


Fig. 5: Block propagation with three nodes.

connected with a high probability. We take this as the basis for our timing analysis. In the following, we will derive our model in detail.

When we assume that the link latency between any two peers follows the same distribution λ and a node’s processing delay can be described as d , then the probability of a time difference t with h edges in between the two reference nodes is given by

$$P(\Delta = t | H = h) = (\lambda^{*h} * d^{*h})(t). \quad (1)$$

Please note that the $*$ -operator denotes a convolution; accordingly, λ^{*h} and d^{*h} denote the h convolution power. To infer the topology, we have to calculate the probability of h edges assuming a time difference t . This is possible using Bayes’ Theorem,

$$P(H = h | \Delta = t) = \frac{P(\Delta = t | H = h) \cdot P(H = h)}{P(\Delta = t)}. \quad (2)$$

The probability that an inventory message arrives after time t , $P(\Delta = t)$, can be calculated according to the law of total probability. The probability $P(\Delta = t | H = h)$ is given by (1). The probability of h edges between the two reference nodes, $P(H = h)$, can be calculated by assuming an Erdős-Rényi random graph model, where the probability of an edge is calculated based on the mean degree. In the case of a mean degree deg and N nodes, the equation is given by

$$P(H = h) = \left[1 - \left(\frac{deg}{N-1} \right) \right]^{h-1} \cdot \left(\frac{deg}{N-1} \right). \quad (3)$$

For our model, we assume that the link latency distribution λ is a result of the three-way message exchange to relay a block. Furthermore, we assume that this latency distribution follows a normal distribution, i.e., $\lambda(x) = \mathcal{N}(x; \mu_\lambda, \sigma_\lambda^2)$. The expected propagation time is presumed to depend on the geolocation of S and R . While this is a very simplifying assumption as latencies may depend on many factors, including AS and peering relationships, country-based measurements are already available and/or easier to obtain in decent quality. The mean μ_λ and variance σ_λ^2 values of the normal distribution can accordingly be estimated by using RTT measurements for

the respective geolocations, multiplied by a factor of 1.5 to mind three-way message exchange.

We define a node's processing delay d as the sum of transmission delay, queuing delay, and block verification time. While the transmission delay can have a significant impact for very large block sizes, we assume the block verification time to be the dominating factor. We therefore assume the network-based delays to be adequately captured by the link latency and leave the development of an advanced transmission model as an open question for future research. Furthermore, we generally assume a linear correlation between the time it takes to validate a new block and the number of included transactions, i.e., the block size s_b . However, since the network peers run on equipment of varying power, the appropriate validation factor is not necessarily a global constant. To account for variations, we model the processing delay d as a normal distribution, i.e., $d(x) = \mathcal{N}(x; \mu_d, \sigma_d^2)$. The resulting function is

$$P(t - \epsilon \leq t \leq t + \epsilon | H = h) = \int_{t-\epsilon}^{t+\epsilon} \mathcal{N}(t; \mu, \sigma^2) dt \quad (4)$$

with $\mu = h \cdot (\mu_\lambda + \mu_d)$, $\sigma^2 = h \cdot (\sigma_\lambda^2 + \sigma_d^2)$. Here ϵ is a tolerance variable adjusting for the possibility of measurement errors. Given the complexity of this model, the selection of reasonable mean and variance values is important to reach an adequate degree of accuracy.

B. Parametrization

The inference model requires a number of parameters which have an impact on the accuracy of the resulting estimations. These parameters include the normal distributions for the latency λ and the processing delay d , as well as the value for the tolerance variable ϵ .

For the latency distribution λ , different data sources are possible. We consider the iPlane dataset [26], which provides publicly available data of global latency measurements, as a viable data source. Admittedly, the data is somewhat outdated but still fits the purpose. It consist of pairs of globally distributed IP addresses and a corresponding RTT value measured on a specific point in time. As an alternative data source, we suggest to conduct ICMP ping measurements from the observation points or to directly utilize the Zcash ping measurements (cf. Fig. 4).

Values for the validation time can also be acquired through different means. We consider the evaluation constant from [7] as a reasonable estimation for μ_d . Unfortunately, in this case we must make some assumptions on the variance. Alternatively, μ_d and σ_d^2 can be acquired experimentally, i.e., by averaging the processing time of a local Zcash node. We compare both approaches in our evaluation.

Varying the tolerance parameter ϵ should generally have no significant influence on the measurement results. However, larger values for ϵ increase the influence of the likelihood $P(t - \epsilon \leq t \leq t + \epsilon | H = h)$ and therefore decrease the influence of the prior probability $P(H = h)$ on the posterior probability.

V. EVALUATION

We evaluate our inference model using two different ways: through a simulation scenario and a real world measurement test with two Zcash nodes.

A. Methodology

In order to facilitate the simulation-based evaluation scenario, we created an undirected graph with a certain amount of vertices utilizing the Boost Graph Library [11]. Every vertex represents a Zcash networking node and creates 8 edges to randomly selected vertices, representing the 8 outgoing connections the reference client tries to establish. The mean degree of the random topology is therefore 16. We assign a country to each vertex and draw an according link latency value for each edge from a normal distribution that was parametrized with the iPlane data set [26]. As discussed before, we multiply this latency value by factor 1.5 to mind the entire three-way message exchange. Moreover, we simulate our vantage point which is connected to all other vertices and therefore able to observe the simulated propagation behavior in its entirety.

Given this network graph, we can deduce simulated time difference measurements by traversing the shortest path between any node and our vantage point, accumulating the edge weights accordingly. In order to retrieve statistically significant results, we repeated this process 50 times for varying edge weights and applied our topology inference model for each of the measurements. Each time, we calculated the probability under a tolerance of $\epsilon = 5ms$ for possible hop counts h of 1 to 9 and finally calculated the mean value for each distance. From this, we deem the value with highest mean probability as the likeliest estimated distance. As we are in full knowledge of the simulated topology, this scenario allows us to exactly determine the precision and recall of our model under the influence of different parametrizations for the processing time distribution $d = \mathcal{N}(x; \mu_d, \sigma_d^2)$ and block sizes s_b . The validation constants k_μ and k_{σ^2} determine the distribution parameters as $\mu_d = k_\mu \cdot s_b$ and $\sigma_d^2 = k_{\sigma^2} \cdot s_b$.

Theoretically, our model could predict the probability of h up to the network diameter. However, our model becomes less accurate for distances above three, since path lengths larger than two exhibit an increased possibility for parallel running paths. Therefore, our model is suited best to infer individual connections one by one. Additionally, as our model utilizes assumptions about the geographic locations of network peers to determine their edge latencies, inaccuracies in the geographic clustering can result in high amount of false positives for certain peer connections. For example, if we assume a scenario in which two nodes located in Germany are connected via a third node located in Russia, our model could predict a distance of five (low latency) edges, even though the simulated path consists only of three (high latency) links.

In our simulation, we considered topologies with 300 nodes, which resembles the measured network size. Furthermore, we evaluate our model in the simulation for distances up to three. For the geographic distribution, we chose two countries each from America and Europe, and three countries from Asia,

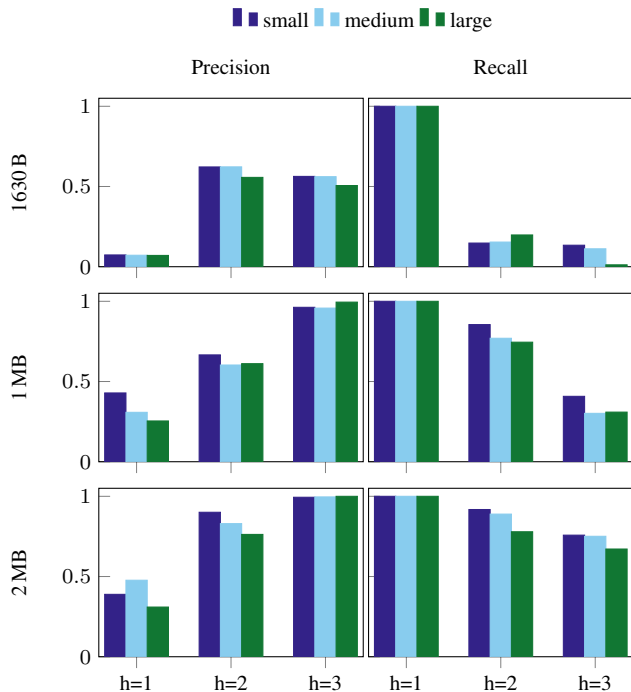


Fig. 6: Precision and Recall for different block sizes, different variances and 300 nodes located in 7 different countries.

whereby we aim to represent the northern Hemisphere. The distribution assigned as follows: 30% United States, 20% in Russia, 10% Canada, 10% China, 10% France, 10% Germany, and 10% Japan.

B. Simulation Results

We use a simulation scenario to evaluate different parametrizations of the processing time distribution d . That is, we evaluated precision and recall of our model for different block sizes s_b assuming the validation constants $k_\mu = 0.3796 \mu s/B$ and $k_{\sigma^2} = 0.552049 \mu s^2/B$ taken from [7]. We also ran the simulations for three different degrees of latency standard deviation: “small”, “medium” and “large”, assuming 10%, 30%, and 50% of the mean, respectively.

The simulation results presented in Fig. 6 show that the model generally performs better with larger block sizes, which yield a precision of up to 40% and recall of up to 100%. Surprisingly, the precision for a direct connection is slightly higher for a 1 MB block than for a 2 MB block. However, the validation time seems to be a good indicator for the number of hops, since the precision for distances two and three are above 50%. Moreover, the larger the block sizes, the higher are the estimated processing times. Hence, the lower is the share of the estimated latency, which makes the model less dependent on accurate latency estimations.

C. Real-World Experiments

In the real-world evaluation scenario, we deployed two nodes in the peer-to-peer network over the course of one week. One node functioned as the measurement node and recorded the arrival time of all block inventory messages. Moreover, as

TABLE I: Real-world measurement results.

	Model of [7]	Test net.	Main net.
k_μ	$0.38 \mu s/B$	$8.55 \mu s/B$	$12.74 \mu s/B$
k_{σ^2}	$0.55 \mu s^2/B$	$345.1 \mu s^2/B$	$2128.16 \mu s^2/B$
True Positive	18	30	33
False Positive	18	26	33
False Negative	22	10	7
Precision	50 %	53.5 %	50 %
Recall	45 %	75 %	82.5 %

a point of reference, the relay node recorded its connections over the time of measurement.

Afterwards, we apply our model to infer if a direct connection between the different block creators and the relay node existed in the given time frame. We calculated RTT estimations using the EWMA approach.

In the measurement period, we estimate the network size to be 316 nodes of which 87 nodes sent at least five blocks. Overall, we recorded 4,160 blocks with an average block size of $15,678 B$ and 21 stale blocks. We also recorded the average validation times our client exhibited during the verification of 5,000 blocks from the Zcash main network. Resulting from this, we set the estimated validation constants to $k_\mu = 12.7357 \mu s/B$ and $k_{\sigma^2} = 2128.16 \mu s^2/B$.

For the further evaluation, we only consider direct connections with the (mining) nodes that announced at least five blocks.

As shown in TABLE I, even despite the low block sizes, our model is able to achieve a precision of 50% and a recall of 82.5% under the discussed parametrization.

D. Discussion

This real-world evaluation scenario shows that we can consider half of the inferred connections as correct and only a small amount of direct connections as missing. The results support the general validity of our inference model. Considering the deliberate simplifying assumptions, the approach seems to be a promising step for inferring the topology of many cryptocurrencies similar to Bitcoin. Furthermore, countermeasures for our method—e.g., artificially delaying block relays—would increase the probability of stale blocks, which weakens the system. It therefore becomes clear that our method will remain usable in the future.

However, it should be possible to improve the precision of the current model by acquiring more diversified latency measurements and considering additional information about the client location, like the AS number. For higher block sizes, a better modeling of the validation time and the transmission delay could also improve the results.

Furthermore, the calculation of the probability of a certain amount of edges between nodes ($P(H = h)$) is calculated based on an Erdős-Rényi model, which is a random topology. However, it is unlikely that nodes are connected randomly in a peer-to-peer network in which certain nodes have a higher uptime than others. It is more likely that some central nodes have more than 16 connections, especially nodes of the core network. We leave these ideas open for future research.

VI. CONCLUSION

In this work, we presented the first longitudinal measurement study of the Zcash peer-to-peer network, revealing key characteristics of the Zcash network. Moreover, we introduced a topology inference model that relies on a passive timing analysis of measured block arrival times. Our evaluation shows that this model allows us to infer node interconnections with a precision of 50 % and recall of 82 % in the real-world scenario. We deem this an attractive approach for passive topology inference of cryptocurrency networks.

REFERENCES

- [1] S. Nakamoto, *Bitcoin: A peer-to-peer electronic cash system*, 2008.
- [2] E. Ben-Sasson, A. Chiesa, C. Garman, M. Green, I. Miers, E. Tromer, and M. Virza, “ZeroCash: Decentralized anonymous payments from bitcoin,” in *SP ’14: Proceedings of the 35th IEEE Symposium on Security and Privacy*, San Jose, CA, USA, May 2014.
- [3] E. Ben-Sasson, A. Chiesa, E. Tromer, and M. Virza, “Succinct non-interactive zero knowledge for a von Neumann architecture,” in *USENIX Security ’14: Proceedings of the 23rd USENIX Security Symposium*, San Diego, CA, USA, 2014, pp. 781–796.
- [4] J. Quesnelle, “On the linkability of zcash transactions,” *ArXiv preprint arXiv:1712.01210*, 2017.
- [5] G. Kappos, H. Yousaf, M. Maller, and S. Meiklejohn, “An empirical analysis of anonymity in zcash,” *ArXiv preprint arXiv:1805.03180*, 2018.
- [6] K. Croman, C. Decker, I. Eyal, A. E. Gencer, A. Juels, A. E. Kosba, A. Miller, P. Saxena, E. Shi, E. G. Sirer, D. Song, and R. Wattenhofer, “On scaling decentralized blockchains - (A position paper),” in *BITCOIN ’16: Proceedings of the 3rd Workshop on Bitcoin Research*, Christ Church, Barbados, Feb. 2016, pp. 106–125.
- [7] A. Gervais, G. Karame, K. Wüst, V. Glykantzis, H. Ritzdorf, and S. Capkun, “On the security and performance of proof of work blockchains,” in *CCS ’16: Proceedings of the 23rd ACM SIGSAC Conference on Computer and Communications Security*, Vienna, Austria, Oct. 2016.
- [8] A. Biryukov, D. Khovratovich, and I. Pustogarov, “Deanonymisation of clients in bitcoin p2p network,” in *CCS ’14: Proceedings of the 21st ACM Conference on Computer and Communications Security*, Scottsdale, AZ, USA, Nov. 2014, pp. 15–29.
- [9] G. C. Fanti and P. Viswanath, “Deanonymization in the bitcoin P2P network,” in *NIPS ’17: Proceedings of 30th Annual Conference on Neural Information Processing Systems*, Long Beach, CA, USA, Dec. 2017.
- [10] T. Neudecker, P. Andelfinger, and H. Hartenstein, “Timing analysis for inferring the topology of the bitcoin peer-to-peer network,” in *UIC ’16: Proceedings of the 2016 International Conference on Ubiquitous Intelligence & Computing*, Toulouse, France, Jul. 2016.
- [11] *Boost graph library*, www.boost.org/doc/libs/1_66_0/libs/graph/doc/, Accessed: 2019-04.
- [12] C. Decker and R. Wattenhofer, “Information propagation in the bitcoin network,” in *P2P ’13: Proceedings of the 13th IEEE International Conference on Peer-to-Peer Computing*, Trento, Italy, Sep. 2013, pp. 1–10.
- [13] G. Pappalardo, T. Di Matteo, G. Caldarelli, and T. Aste, “Blockchain inefficiency in the bitcoin peers network,” *EPJ Data Science*, vol. 7, no. 1, p. 30, 2018.
- [14] S. K. Kim, Z. Ma, S. Murali, J. Mason, A. Miller, and M. Bailey, “Measuring ethereum network peers,” in *IMC ’18: Proceedings of the Internet Measurement Conference*, Boston, MA, USA, Oct. 2018, pp. 91–104.
- [15] A. E. Gencer, S. Basu, I. Eyal, R. van Renesse, and E. G. Sirer, “Decentralization in bitcoin and ethereum networks,” in *FC ’18: Proceedings of the 22nd International Conference on Financial Cryptography and Data Security*, Santa Barbara, Curaçao, Feb. 2018.
- [16] B. Kaiser, M. Jurado, and A. Ledger, “The looming threat of china: An analysis of chinese influence on bitcoin,” *CoRR*, vol. abs/1810.02466, 2018.
- [17] M. Coates, R. M. Castro, R. D. Nowak, M. Gadhiok, R. King, and Y. Tsang, “Maximum likelihood network topology identification from edge-based unicast measurements,” in *SIGMETRICS ’02: Proceedings of the International Conference on Measurements and Modeling of Computer Systems*, Marina Del Rey, California, USA, Jun. 2002, pp. 11–20.
- [18] T. Shirai, H. Saito, and K. Taura, “A fast topology inference: A building block for network-aware parallel processing,” in *HPDC ’07: Proceedings of the 16th International Symposium on High-Performance Distributed Computing*, Monterey, California, USA, Jun. 2007, pp. 11–22.
- [19] N. G. Duffield, J. Horowitz, F. L. Presti, and D. Towsley, “Multicast topology inference from measured end-to-end loss,” *IEEE Transactions on Information Theory*, vol. 48, no. 1, pp. 26–45, 2002.
- [20] A. Miller, J. Litton, A. Pachulski, N. Gupta, D. Levin, N. Spring, and B. Bhattacharjee, *Discovering bitcoin’s public topology and influential nodes*, May 2015.
- [21] M. Grundmann, T. Neudecker, and H. Hartenstein, “Exploiting transaction accumulation and double spends for topology inference in bitcoin,” in *BITCOIN ’18: Proceedings of the 5th Workshop on Bitcoin Research*, Santa Barbara, Curaçao, Feb. 2018.
- [22] T. Neudecker and H. Hartenstein, “Network layer aspects of permissionless blockchains,” *IEEE Communications Surveys and Tutorials*, vol. 21, no. 1, pp. 838–857, 2019.
- [23] T. Neudecker, “Characterization of the bitcoin peer-to-peer network (2015-2018),” Karlsruhe, Tech. Rep. 1, 2019, 29 pp.
- [24] *Zcash - network*, z.cash/upgrade/, Accessed: 2019-05.
- [25] *Maxmind*, www.maxmind.com/, Accessed: 2019-03.
- [26] *iPlane: An information plane for distributed services*, web.eecs.umich.edu/~harshavm/iplane/, Accessed: 2019-04.